A New LLC Resonant Converter with Multiple Outputs for High Efficiency and Low Cost PDP Power Module

Chong-Eun Kim*, Kang-Hyun Yi*, Gun-Woo Moon*, Buem-Joo Lee**, and Sang-Man Kim**

Korea Advanced Institute of Science and Technology (KAIST)*
DANAM communications Inc.**

Abstract

A new LLC resonant converter with multiple outputs is proposed for high efficiency and low cost plasma display panel (PDP) power module. In the proposed converter, ZVS turn-on of the primary MOSFETs and ZCS turn-off of the secondary diodes are guaranteed in the overall input voltage and output load range. Moreover, the primary MOSFETs and the secondary diodes have low voltage stresses clamped to input and the output voltage, respectively. Therefore, the proposed converter shows the high efficiency due to the minimized switching and conduction losses. In addition, by employing the transformer, which has the two and more secondary side, the proposed converter can have multiple outputs and they show the great cross-regulation characteristics. As a result, the proposed converter can be implemented with low cost and compact size. The 500W prototype is implemented, which integrates the sustaining and addressing power supplies of PDP power module. The maximum efficiency is 96.8% and the respective output voltages are well regulated. Therefore, the proposed converter is suitable for high efficiency and low cost PDP power module.

1. Introduction

PDPs show the desired features as the display device, such as large screen size, wide view angle, fast response, high contrast, thinness, and long life time. Moreover, recently, the power consumption is decreased through the auto power control (APC) technique, and the cost per inch is reduced through the application-specific integrated circuit (ASIC) technology and the improvement of the panel fabrication process. Therefore, PDPs show the brightest prospect as the flat display panel.

PDPs operate in three periods of resetting, addressing, sustaining, in order to display the desired images. In resetting period, the wall charges of the overall PDP cells are removed by applying the resetting ramps to the scanning and sustaining electrodes. And then, to create wall charges at the required PDP cells, the data and scanning pulses are applied to the addressing and scanning electrodes, respectively. If the continuous sustaining pulses are applied between the scanning and sustaining electrodes during the sustaining period, the selected PDP cells emit the strong light and the desired image is displayed. Therefore, to drive PDPs optimally, the various power supplies are required, such as the sustaining, addressing, scanning, and resetting power supplies.

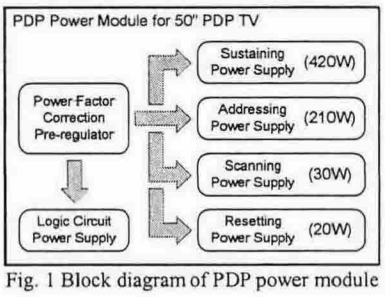

Fig. 1 Block diagram of PDP power module

PDP power module includes not only these required power supplies but the logic circuit power supply, as shown in Fig. 1. In addition, the boost pre-regulator for power factor correction (PFC) is implemented at input stage. PDP power module has the complicated structure and the high power rating, especially, of the sustaining and addressing power supplies. However, as described above, the sustaining and addressing power supplies are utilized not simultaneously but alternatively.

Therefore, the sustaining and addressing power supplies can be implemented as single power stage with multiple outputs and then PDP power module can have the high power density and the low cost.

In this paper, a new LLC resonant converter suitable for multiple outputs is proposed. The operational principles are analyzed and the cross-regulation characteristics for multiple outputs are investigated. Moreover, the 420W prototype of the proposed converter is implemented for the sustaining and addressing power supplies and its operations and performances are investigated.

2. Principles of Operation

As shown in Fig. 2, the proposed converter consists of two half-bridge cells as the input and output stages, symmetrically. The input and the output stages are connected by the resonant cell, which is composed of the series resonant inductor L_R, the series resonant capacitor C_R, and the transformer T_1. Moreover, the transformer includes the magnetizing inductor L_M, and it works as the parallel resonant inductor.

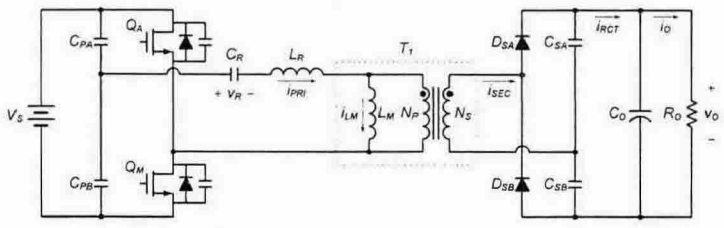

Fig. 2 Circuit diagram of the proposed converter

A. Mode analysis

The proposed converter operates in six modes according to the switching states of the primary MOSFETs and the secondary diodes, and the key waveforms are presented in Fig. 3. Before t_0, since D_{SA} and D_{SB} are turned-off, the transformer secondary current i_{SEC} is zero. The transformer primary current i_{PRI} flows reversely through Q_A and it equals to the transformer magnetizing current i_{LM}.

When Q_A is turned-off at t_0, mode 1 begins. Since i_{PRI} has the negative current, it discharges the parasitic output capacitor of Q_M and charges that of Q_A. Provided that the firing signal is applied to Q_M after the parasitic output capacitor of Q_M is fully discharged, ZVS turn-on is obtained. And mode 2 begins at t_1. In mode 2, D_{SA} is turned-on and i_{LM} is increased by the applied voltage of $(1/2)V_O$. Simultaneously, L_R and C_R resonate with the applied voltage of $(1/2)(V_S-V_O)$, as shown in Fig. 2. When i_{PRI} becomes equal to i_{LM}, D_{SA} is turned-off and mode 3 begins at t_2. L_M, L_R, and C_R resonate with the applied voltage of by $(1/2)V_S$, and i_{PRI} equals to i_{LM} in mode 3. When Q_M is turned-off at t_3, mode 4 begins. The operations of mode 4, 5, and 6 are symmetrically same as those of mode 1, 2, and 3, respectively.

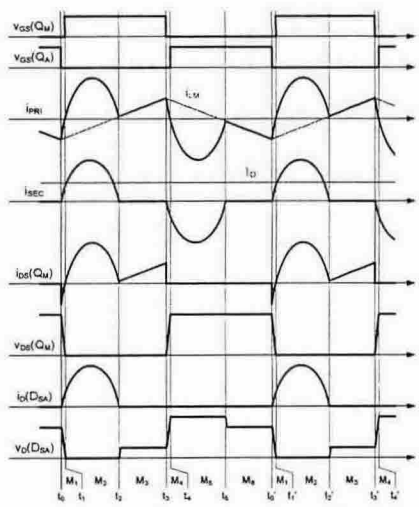

Fig. 3 Key waveforms of the proposed converter

B. Input-output voltage gain

Using the fundamental component simplification (FCS) method, we can drive the input-output voltage gain of the proposed converter given by

$$G_{DC} = \frac{V_O}{V_S} = \frac{\frac{N_S}{N_P}}{\sqrt{\left\{1+k\left[1-\left(\frac{F_R}{F_S}\right)^2\right]\right\}^2 + \left[\left(\frac{F_S}{F_R}-\frac{F_R}{F_S}\right)Q\right]^2}}, \quad (1)$$

where

$$F_R = \frac{1}{2\pi\sqrt{L_R C_R}}, \quad (2)$$

$$Q = \sqrt{\frac{L_R}{C_R}}\frac{1}{R_{ac}}, \quad (3)$$

$$R_{ac} = \frac{2}{\pi^2}\left(\frac{N_P}{N_S}\right)^2 R_O, \quad (4)$$

$$k = \frac{L_R}{L_M}, \quad (5)$$

and F_S is the switching frequency. In Fig. 4, the input-output voltage gain is plotted as the function of the ratio F_S to F_R, with the circuit parameters of L_R=12μH, L_M=220μH, C_R=100nF, N_P:N_S=1:1.

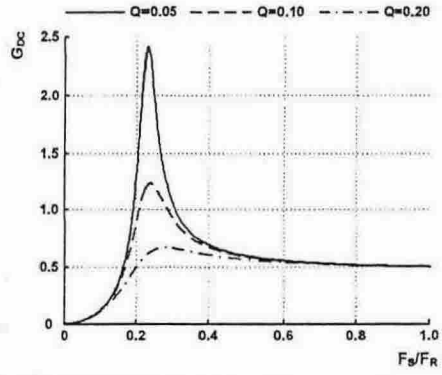

Fig. 4 Input-output voltage gain of the proposed converter

3. Cross-Regulation Characteristics

For double outputs, the circuit diagram of the proposed converter is shown in Fig. 5. The transformer T_1 consists of one primary side and two secondary sides. In addition, the secondary sides have the respective leakage inductances.

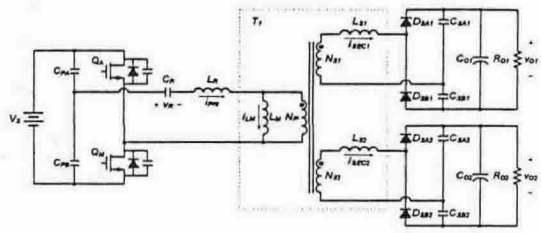

Fig. 5 Circuit diagram for double outputs

A. Ideal case

Provided that the leakage inductances of the transformer secondary sides are zero, the respective the input-output voltage gains can be derived using the FCS method as the following equations.

$$G_{DC1} = \frac{V_{O1}}{V_S} = \frac{\frac{N_{S1}}{N_P}}{\sqrt{\left\{1+k\left[1-\left(\frac{F_R}{F_S}\right)^2\right]\right\}^2 + \left[\left(\frac{F_S}{F_R}-\frac{F_R}{F_S}\right)Q\right]^2}}, \quad (6)$$

$$G_{DC2} = \frac{V_{O2}}{V_S} = \frac{\frac{N_{S2}}{N_P}}{\sqrt{\left\{1+k\left[1-\left(\frac{F_R}{F_S}\right)^2\right]\right\}^2 + \left[\left(\frac{F_S}{F_R}-\frac{F_R}{F_S}\right)Q\right]^2}}, \quad (7)$$

where

$$R_{ac} = R_{O1,ac} // R_{O2,ac}, \quad (8)$$

$$R_{O1,ac} = \frac{2}{\pi^2}\left(\frac{N_P}{N_{S1}}\right)^2 R_{O1}, \quad (9)$$

$$R_{O2,ac} = \frac{2}{\pi^2}\left(\frac{N_P}{N_{S2}}\right)^2 R_{O2}. \quad (10)$$

The ratio of the input-output voltage gains equals exactly to the turns ratio of the transformer secondary sides, irrespective of the other conditions. Therefore, the cross-regulation of both the outputs is guaranteed in the ideal case.

B. Non-ideal case

Practically, the transformer has the leakage inductances in the secondary sides as well as the primary side. Therefore, the input-output voltage gains, presented in the equations (6) and (7), cannot be applicable. Similarly, using the FCS method with the secondary leakage inductor L_{S1} and L_{S2}, we can derive the input-output voltage gains of practical case as follows.

$$G_{DC1} = \frac{V_{O1}}{V_S} = \frac{N_{S1}}{N_P} \frac{R_{O1}/\pi^2}{\sqrt{\left(R_{O1}/\pi^2\right)^2 + \left(\pi L_{S1} F_S\right)^2}} G_{COM}, \quad (11)$$

$$G_{DC2} = \frac{V_{O2}}{V_S} = \frac{N_{S2}}{N_P} \frac{R_{O2}/\pi^2}{\sqrt{\left(R_{O2}/\pi^2\right)^2 + \left(\pi L_{S2} F_S\right)^2}} G_{COM}, \quad (12)$$

where G_{COM} is given by the equation (16),

$$\alpha = \frac{\pi^4}{4} \frac{L_{S1}}{R_{O1}} \frac{L_{S2}}{R_{O2}}, \quad (13)$$

$$\beta = \frac{\pi^2}{2} \left(\frac{L_{S1}}{R_{O1}} + \frac{L_{S2}}{R_{O2}} \right), \quad (14)$$

$$\gamma = \frac{\pi^4}{4} \frac{1}{R_{O1} R_{O2}} \left(\frac{L_{S1}}{N_{S1}} + \frac{L_{S2}}{N_{S2}} \right) \left(\frac{N_{S1} N_{S2}}{N_P} \right)^2. \quad (15)$$

Different from the ideal case, the ratio of the input-output voltage gains is not equal to the turns ratio of the transformer secondary sides, and it is affected not only by the turns ratio but by the leakage inductances and the load resistances. The input-output voltage gains are plotted in Fig. 6 as the functions of the load resistances with the circuit parameters of L_R=12μH, L_M=220μH, C_R=100nF, F_S=100kHz, and N_P: N_{S1}:N_{S2}=23:12:4.

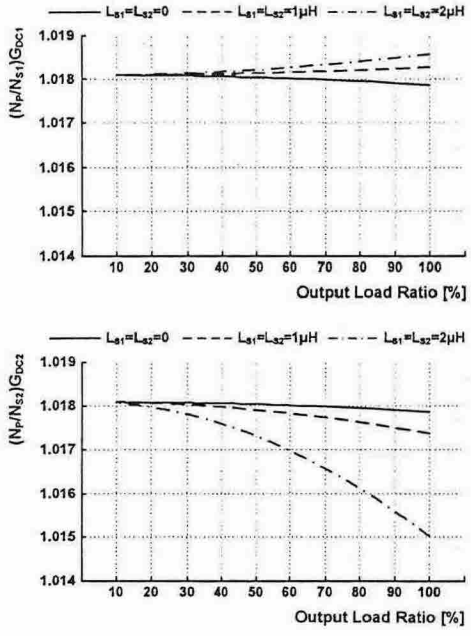

Fig. 6 Input-output voltage gains as the functions of the output load ratio

4. Experimental Results

To verify the operational principles and the cross-regulation characteristics of the proposed converter, the 420W prototype is implemented for the sustaining and addressing power supplies of PDP power module. In Fig. 7, the key current waveforms are shown at both 100% and 10% output load condition, and they are well agreed to the theoretical waveforms. The cross-regulation characteristics at the static load condition are investigated and the addressing output voltage as the function of the sustaining output current is plotted in Fig. 8. The maximum variation of the addressing output voltage is measured to 1.07V (1.6%) and this is reasonable.

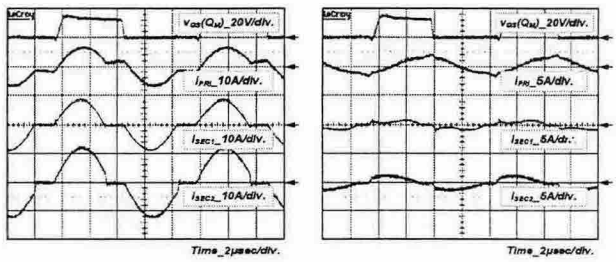

Fig. 7 Key experimental current waveforms

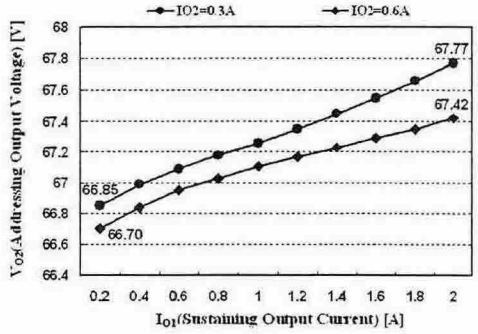

Fig. 8 Cross-regulation at the static load condition

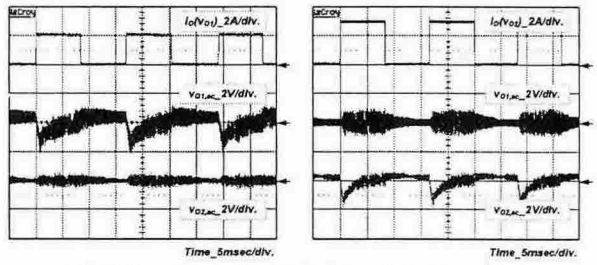

Fig. 9 Cross-regulation at the dynamic load condition

Furthermore, the cross-regulation characteristics at the dynamic load condition are examined. The resulting waveforms are presented in Fig. 9 and the maximum variation of both the outputs is 2V or below. In addition, the implemented prototype has the maximum efficiency of 96.8% at the full load condition.

5. Conclusions

In this paper, a new LLC resonant converter with multiple outputs is proposed for high efficiency and low cost PDP power module. The operational principles of the proposed converter are analyzed and the cross-regulation characteristics for multiple outputs are investigated. Moreover, the 420W prototype of the proposed converter is implemented for the sustaining and addressing power supplies and its operations and performances are confirmed. The proposed converter is expected to be suitable for the high efficiency and low cost PDP power module and other multi-output applications.

Acknowledgement

This work was supported (in part) by the Ministry of Information & Communications, Korea, under the Information Technology Research Center (ITRC) Support Program.

$$G_{COM} = \frac{\left(1 - 4\pi^2 \alpha F_S^2\right)^2 + 4\pi^2 \beta^2 F_S^2}{\sqrt{\left[1 + k\left(1 - \frac{F_R^2}{F_S^2}\right) + 4\pi^2 k\alpha\left(F_R^2 - F_S^2\right) + \frac{\alpha}{C_R} - 4\pi^2 L_P \gamma F_S^2\right]^2 + \left[\left(\frac{F_S}{F_R} - \frac{F_R}{F_S}\right)Q + \left(k\frac{F_S}{F_R} - \frac{F_R}{F_S}\right)2\pi\beta F_R\right]^2}} \quad (16)$$